Contents

1
Ultracold Fermi Gases: Properties and Techniques

Selim Jochim

1.1
Introduction

After Fermi and Dirac had formulated their statistics for half-integer spin particles in 1926 it was immediately applied to Fermi gases such as neutron stars, or the electron gas in metals. But only significantly later, Bardeen, Cooper and Schrieffer (BCS) were able to explain superconductivity by a weak attractive interaction among the electrons that form delocalized Cooper pairs in momentum space. Due to their very weak coupling, superconductivity in BCS-type superconductors only occurs at extremely low temperatures, way below the Fermi temperature of the electron gas, limiting their practical use. When in 1986, G. Bednorz and A. Müller found superconductivity at temperatures as high as 35 K (high-T_C), applications of superconductivity in everyday life suddenly became much more realistic. However, until now, solid state physics theory is not capable to fully explain the complex processes that lead to such high critical temperatures.

Ultracold atomic Fermi gases offer a number of major advantages that contribute significantly to getting a better understanding of the many-body physics of fermions. First of all, due to the extremely low densities and temperatures in ultracold gases, interactions between the particles can typically be described by one single parameter, the *s*-wave scattering length *a*. As for identical fermions *s*-wave scattering is forbidden because of their antisymmetric properties, one can even create a completely noninteracting ideal Fermi sea. In most cases however, we would like the trapped fermions to interact with each other which can be realized in the simplest way by preparing the atoms in a mixture of different internal spin states. In most of the experiments described in this chapter, we are dealing with a spin mixture of two Zeeman states of the same atom, analogous to the spin up and down mixture that exists in an electron gas.

The interaction between the trapped particles due to typical scattering lengths is very weak, so that superfluidity in ultracold Fermi gases is predicted to occur at very low temperatures, out of reach for current experiments. Luckily, a great opportunity to tune the scattering length to arbitrary values by applying an external magnetic field near so-called Feshbach resonances has emerged in recent years. While the details of the interatomic potentials can still be neglected, the interaction strength can be tuned to arbitrary values. In fact, just at the resonance position, a new molecular bound state is introduced. It turned out that it is possible to start with a weakly interacting ultracold gas of atoms, and by simply changing the magnetic field first obtain a strongly interacting Fermi gas, before one finally ends up with a gas of bosonic molecules that form a Bose-Einstein condensate (BEC). What happens in between is the so-called BCS-BEC crossover, that smoothly converts a gas of fermions into bosons! One of the major findings is that a Fermi gas with resonant interactions can have a critical temperature higher than a tenth of the Fermi temperature, much higher than any currently known high-T_C superconductor.

In this chapter we will first discuss the properties of ultracold fermions in a harmonic trap and how to prepare such a gas. Then we will discuss the effect of interactions and how they can be altered using a Feshbach resonance. An important topic will be the creation of molecules and molecular condensates as a starting point for experiments with strongly interacting gases in the BCS-BEC crossover. We assume that the reader has basic knowledge of ultracold collisions and BECs as they are the topic of previous chapters in this book.

1.2 Ultracold Fermions in a Trap

All traps that we will be considering in this chapter can be approximated by a harmonic potential at the trap center, such that we can write the trapping potential as

$$V(\vec{r}) = \frac{1}{2}m\omega_x^2 x^2 + \frac{1}{2}m\omega_y^2 y^2 + \frac{1}{2}m\omega_z^2 z^2, \tag{1.1}$$

where m is the mass of the atoms, and $\omega_x/2\pi$, $\omega_y/2\pi$, $\omega_z/2\pi$ are the trap frequencies in the respective axes of the trap. For many calculations it will be sufficient to consider without loss of generality a spherically symmetric trap with a mean trap frequency

$$\bar{\omega} = \left(\omega_x\omega_y\omega_z\right)^{1/3}. \tag{1.2}$$

1.2.1 Ideal Fermi Gas

Because *s*-wave collisions are forbidden for identical Fermions (see Sec. 1.4.1), a spin polarized gas of Fermions is essentially non-interacting at ultralow temperatures. The absence of interactions in such a gas makes its description relatively simple. Here we summarize quickly the properties of such a gas in a harmonic trap, and look only at the thermodynamic limit, where the particle number is large. This allows us to ignore the quantization of the trapping potential and we can use the Fermi distribution function in the form

$$f(\vec{r},\vec{p}) = \frac{1}{\exp((\vec{p}^2/2m + V(\vec{r}) - \mu)/k_B T) + 1} \tag{1.3}$$

where the chemical potential μ is constrained by the number of particles as

$$N = \frac{1}{(2\pi\hbar)^3}\int f(\vec{r},\vec{p})\, d\vec{r}\, d\vec{p} = \frac{1}{2(\hbar\bar{\omega})^3}\int_0^\infty \frac{E^2\, dE}{\exp((E-\mu)/k_B T)+1}, \tag{1.4}$$

where for the second half of the equation the harmonic potential of Eq. 1.1 is assumed. At $T = 0$, the integral just counts all the number of occupied quantum states in the trap, and one obtains

$$\mu(T=0) = (6N)^{1/3}\hbar\bar{\omega} \equiv E_F \equiv k_B T_F, \tag{1.5}$$

which we use as the definition for the Fermi energy and the Fermi temperature. In this semiclassical approximation we can also readily calculate the the density and momentum distributions of the noninteracting gas at zero temperature, by simply integrating the distribution function over $\vec{p}$ or $\vec{r}$, respectively. The results are

$$\begin{aligned} n(\vec{r}) &= \frac{1}{6\pi^2\hbar^3}\left(2m(E_F - V(\vec{r}))\right)^{3/2} \\ &= \frac{8}{\pi^2}\frac{N}{x_F y_F z_F}\left(1 - \frac{x^2}{x_F^2} - \frac{y^2}{y_F^2} - \frac{z^2}{z_F^2}\right)^{3/2} \end{aligned} \tag{1.6}$$

and

$$\begin{aligned} n(\vec{p}) &= \frac{1}{(2\pi\hbar)^3}\int \Theta\left(\frac{p^2}{2m} + V(\vec{r}) - E_\mathrm{F}\right)\, d\vec{r} \\ &= \frac{8}{\pi^2}\frac{N}{p_\mathrm{F}^3}\left(1 - \frac{p^2}{p_\mathrm{F}^2}\right)^{3/2}. \end{aligned} \tag{1.7}$$

Obviously, these equations are valid where they are positive, while outside this range, they are both zero. In the final form of these equations we have

used the Fermi radii and momenta defined as:

$$E_F = \frac{1}{2}m\omega_x^2 x_F^2 = \frac{1}{2}m\omega_y^2 y_F^2 = \frac{1}{2}m\omega_z^2 z_F^2 = \frac{p_F^2}{2m}. \tag{1.8}$$

Note that while the spatial distribution depends on the trap frequencies of the individual axes, the momentum distribution is always isotropic for a noninteracting Fermi gas, independent of the trapping potential.

Finite Temperature To obtain density or momentum distributions at finite temperatures, we have to integrate Eq. 1.3, as before. But as we cannot give an explicit expression for the chemical potential μ, the results can only be given in terms of a polylogarithmic function,

$$Li_n(x) = \frac{1}{\Gamma(n)}\int \frac{t^{n-1}dt}{\exp(t)/x + 1} = \sum_{k=1}^{\infty} x^k/k^n, \tag{1.9}$$

where the second identity is very useful, when such a function needs to be integrated, for example to calculate an integrated 2-D or 1-D density distribution. The result for the density and momentum distributions is

$$n(\vec{r}) = -\left(\frac{mk_BT}{2\pi\hbar^2}\right)^{3/2} Li_{3/2}\left(-\exp\left(\frac{\mu - V(\vec{r})}{k_BT}\right)\right) \tag{1.10}$$

and

$$n(\vec{p}) = -\frac{1}{\hbar^3\omega_x\omega_y\omega_z}\left(\frac{k_BT}{2\pi}\right)^{3/2} Li_{3/2}\left(-\exp\left(\frac{\mu - \vec{p}^2/2m}{k_BT}\right)\right). \tag{1.11}$$

As before, we assumed a harmonic potential of the type 1.1 for the calculation of Eq. 1.11. Again, it can be seen that while the density distribution is dependent on the trapping potential, while the momentum distribution is isotropic.

Chemical Potential To plot now any of these two equations for as specific temperature, one still needs to know the associated chemical potential. In fact most thermodynamic quantities require the knowledge of the chemical potential. For a Fermi gas in a trap at finite temperature it cannot be evaluated analytically. But we can find a rather simple numerical solution. We start by integrating equation 1.4. It can be written as

$$N = -\left(\frac{k_BT}{\hbar\bar{\omega}}\right)^3 Li_3\left(-\exp\left(\frac{\mu}{k_BT}\right)\right). \tag{1.12}$$

Using equation 1.5 we can replace $N(\hbar\bar{\omega})^3$ by $(k_BT_F)^3/6$, and obtain an equation that constrains μ only by T and T_F:

$$Li_3\left(-\exp\left(\frac{\mu}{k_BT}\right)\right) = -\frac{1}{6(T/T_F)^3}. \tag{1.13}$$

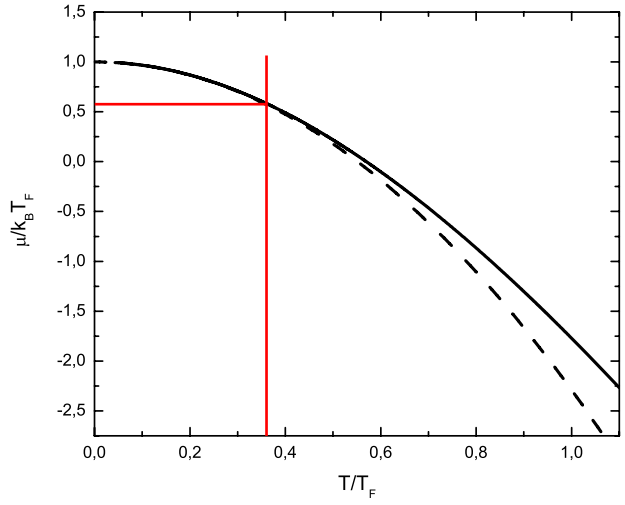

Fig. 1.1 Chemical potential μ of a noninteracting Fermi gas in a harmonic trap with respect to the temperature. Both quantities are normalized to the Fermi temperature T_F. The solid curve represents a numerical calculation according to Eq. 1.13, the dashed line is the Sommerfeld expansion, which is valid for small T/T_F.

This equation represents a universal relationship between the chemical potential and the temperature in terms of the Fermi temperature, independent of the trap parameters, or the number of particles in the trap. However, this relation has to be solved numerically for $\mu = \mu(T/T_F)$. The result of the numerical solution is shown as the solid line in figure 1.1.

For very low temperatures $T \ll T_F$, we can approximate the chemical potential by expanding it in terms of T/T_F. This is the so-called Sommerfeld expansion [10],

$$\mu(T) = E_F \left[1 - \frac{\pi^2}{3} \left(\frac{T}{T_F} \right)^2 \right], \tag{1.14}$$

in which higher order terms vanish for a harmonic potential. For comparison, this equation is plotted as a dashed line in figure 1.1 together with the exact result. For relatively high temperatures $T \geq T_F$, the classical expression for the chemical potential is a good approximation. In terms of T/T_F, it can be expressed as [10]

$$\mu(T) = -k_B T \ln \left[6 \left(\frac{T}{T_F} \right)^3 \right]. \tag{1.15}$$

Knowing $\mu(T/T_F)$, we can now proceed to plot the density distributions for various temperatures as shown in Fig. 1.2. Note that for our harmonic

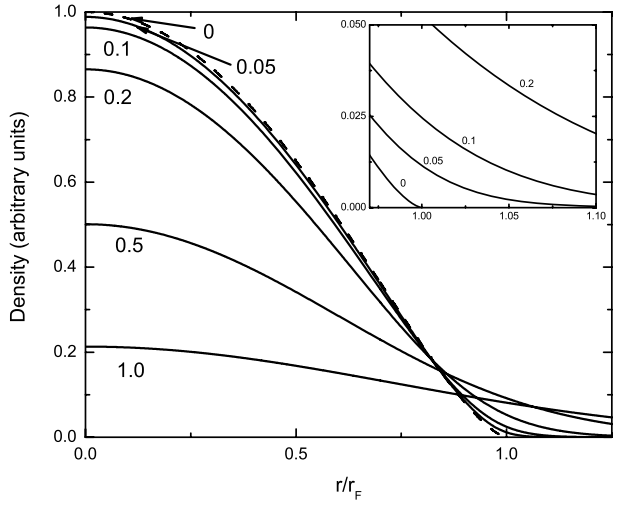

Fig. 1.2 Density distribution of a noninteracting Fermi gas in a harmonic trap for various temperatures T/T_F. The inset shows the region near the Fermi radius. Only here, there is a significant difference in density for highly degenerate gases. Note that the relative density scale of the inset only extends to 5 % of the maximum intensity

trap, density and momentum distributions have the same shape: Just replace the r/r_F by p/p_F on the abscissa. The inset of Fig. 1.2 shows that for temperatures much smaller than the Fermi temperature, it is actually very hard to make out a difference from the $T = 0$-profile, making it especially difficult to fit a temperature to a measured density distribution. The edge of the momentum distribution at p_F of a highly degenerate Fermi gas is called the Fermi surface, which is softened by thermal excitations. As deeply inside the Fermi sphere, all quantum states are occupied, collisions can only occur near the Fermi surface, because inside, Pauli blocking does not allow particle to change their momentum state. Therefore, a weakly interacting Fermi gas is completely collisionless except for atoms near the Fermi surface.

1.3 Preparing an Ultracold Fermi Gas

Many of the techniques and methods needed to trap and cool fermions had already been developed for Bose gases and were described in the previous chapters. Therefore we only enumerate the major steps here and point out the particularities. So far, all experiments on ultracold Fermi gases use a magne-

tooptical trap as a source for cold atoms, which restricts the available species to those fermionic isotopes that can be laser cooled with a reasonable effort. Thus, most of the current experiments use either ^{40}K [19] and ^{6}Li [63], while metastable $^{3}He^{*}$ [44] and ^{173}Yb [24] have also been cooled to degeneracy more recently.

For further evaporative cooling, both magnetic and optical traps are employed. As in magnetic traps the trapping potential depends on the magnetic moments, it is not independent of the internal state of the atoms. This is a serious drawback as in most experiments mixtures of different spin states are used. This is why most current setups use optical traps at least for the final stage of cooling and for experiments. In far off-resonant optical dipole traps, the atoms are trapped by the electric polarizability, independent of their Zeeman sublevel at sufficient detuning. Furthermore, optical traps provide a lot of flexibility in shaping the trapping potential. A detailed overview of dipole traps is given in [28].

The first obstacle that one faces in preparing a degenerate Fermi gas is the lack of *s*-wave collisions in a spin polarized gas, which are a necessary prerequisite for thermalization during evaporative cooling. And so far, no real alternative techniques to evaporative cooling exist. Therefore all experiments working have used a mixture of non-identical particles for the preparation of their degenerate gas. Three different methods are employed in current experiments:

- Non-identical particles can simply be two different spin states of the same atoms, as it has been done in the first realization of a degenerate Fermi gas with ^{40}K-atoms [19]. The major advantage of this technique is that it does not require laser cooling of more than one species as is necessary for all other techniques. This method has gained a lot of popularity later when cooling ^{6}Li with resonantly tuned elastic collisions using a Feshbach resonance proved to work extremely well [26, 38].

- Using bosonic atoms as a cooling agent for the Fermions is an attractive technique as these bosons can also collide among each other, and therefore, more efficient evaporative cooling can be expected. If one uses a bosonic isotope of the same species, due to the relatively small isotope shift, ($\sim$ 10 GHz for Lithium) the same technology, or even the same laser system can be used to laser cool both isotopes [45].

- The largest Fermi gases to date are being prepared using bosonic Sodium as a cooling agent. The major advantage here is that very large cold ensembles of Sodium can be made, enabling a very high cooling efficiency.

Several Spin States The first degenerate Fermi gas was produced in a mixture of the $F = 9/2$, $m_F = 7/2, 9/2$ states of ^{40}K in a magnetic trap, in which

the atoms were cooled by forced radio frequency evaporation [19], similar to how most BECs are prepared. The crucial difference is however, that in this case, one is dealing with two noninteracting ensembles in the two spin states, that reach thermal equilibrium only through thermal contact with each other. To ensure that thermal equilibrium is maintained during evaporative cooling, the amount of atoms in both states has to be closely matched by simultaneously removing atoms from both spin states. In the case of the above mentioned experiment this was achieved by applying two separate radio frequencies for the two spin states. When the gas approaches degeneracy, momentum can only be exchanged with atoms near the Fermi surface of each state. This makes it indispensable that the surfaces of the two states are matched adequately, which obviously is getting more and more difficult to achieve when the gas becomes more and more degenerate.

The technique of using two spin states that sympathetically cool each other becomes considerably simpler, when the two states are trapped by the same potential and experience the same evaporation threshold. These requirements are easily fulfilled in a far detuned optical trap, a concept that was first adopted by John Thomas and his group [26]. Such a far detuned trap confines the atoms independent of their spin state, and forced evaporation causes both states to be removed equally. When the interactions between the particles are tuned resonantly, and pairing occurs, this method also ensures an equal spin mixture, as unpaired atoms are evaporated much more efficiently from the trap, and eventually one is left with a pure paired sample.

Different Isotopes Many of the difficulties described above for evaporative cooling of a spin mixture of one kind of atoms are eased if one uses a bosonic gas as a coolant for the Fermi gas. In this case the basic idea is that the bosonic isotope will be cooled in much the same way as for the preparation of a Bose-Einstein condensate. At the same time it will serve as a thermal bath for the Fermions confined in the same trap. Most easily this is achieved by simply choosing a bosonic isotope of the same atom, such as ^{40}K-^{41}K, or ^{6}Li-^{7}Li, because the same, or similar laser systems can be used for laser cooling of both isotopes: While the isotope shift requires slightly different laser frequencies, they are typically well within the tuning range of any laser source that might be used.

The first success using this concept was reported by the groups of Randy Hulet and Christophe Salomon [60, 63], who sympathetically cooled ^{6}Li using the bosonic isotope ^{7}Li as a coolant. One very beautiful aspect of these experiments was that the properties of a Bose gas could be directly compared to those of a Fermi gas of the same type of atoms, while the two gases cooled down simultaneously. What happened is shown in Fig. 1.3: As the two gases approach degeneracy, the bosonic cloud shrinks rapidly while the size of the

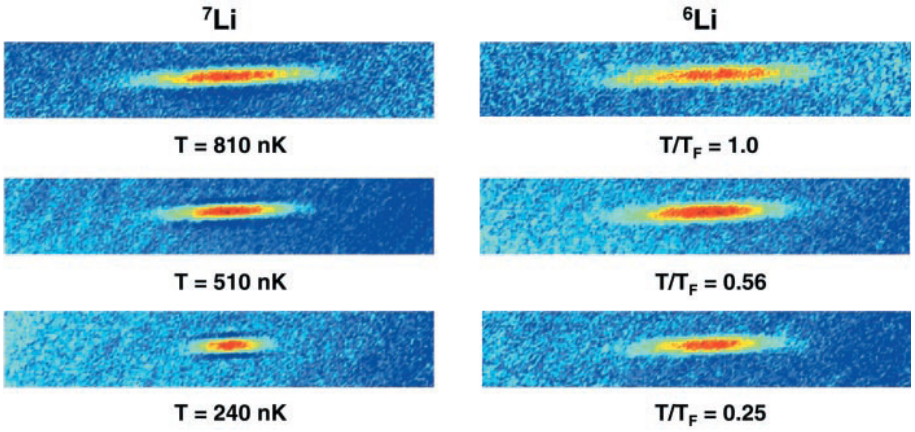

Fig. 1.3 Observation of Fermi pressure: During evaporative cooling the bosonic cloud of ^7Li atoms shrinks significantly as the temperature is lowered while the fermionic cloud of ^6Li atoms does not shrink very much as the gas is cooled deeper into degeneracy. From Science **291**, 2570. Reprinted with permission from AAAS.

Fermi sea does not shrink notably any more. Higher and higher signal-to-noise is required to measure directly the temperature of the Fermi gas that is being cooled below the Fermi temperature, as it differs less and less in shape from an ideal Fermi gas at zero temperature. The shrinking cloud of bosonic atoms that is in thermal contact with the Fermi sea can serve as a precise thermometer in this case. However, using ^7Li has a serious disadvantage: As its s-wave scattering length is negative, only a limited number of Bose-condensed atoms can exist [7]. This limits the number of atoms that can serve as a coolant, and thereby the specific heat available for cooling the Fermions is limited when the samples become deeply degenerate.

Different Atoms If one aims for a very large number of degenerate Fermions, one would want a bosonic coolant that can be readily obtained in large numbers, and that exhibits more favorable scattering properties, such that large Bose-Einstein condensates can be produced. This means that Sodium [30] and Rubidium [56, 61] are a natural choice as a coolant. As both of them do not have a fermionic isotope, it becomes necessary in this case to set up two atom sources, and two laser systems for cooling the two species, increasing significantly the experimental effort. But indeed the largest fermi seas are created in this way, containing up to 10^8 degenerate Lithium atoms [29].

Very Low Temperatures: Overcome Pauli Blocking One other important difficulty of cooling a Fermi gas when it approaches degeneracy is a phenomenon called Pauli-blocking. As the gas is cooling down, only particles with a mo-

mentum that is close to the Fermi sphere can collide and contribute to thermalization. All the atoms deep inside the Fermi sphere cannot be scattered into a new momentum state, because all accessible states are already occupied by identical Fermions. This effect was studied carefully in Ref. [20]. Obviously, this challenge becomes more and more important as the gas is being cooled well below the Fermi temperature, and the width of the Fermi sphere becomes smaller.

The suppression of elastic collisions causes evaporative cooling rates to drop significantly. Thus, successful evaporative cooling then relies on very low inelastic collision rates, and extremely stable trapping potentials, that on one hand are deep enough to confine the Fermi sea with its maximum energy E_F, and on the other hand, feature a stability both in depth as well as in position that causes heating rates to be small enough to match the small evaporative cooling rates that can be achieved in a highly degenerate Fermi gas.

An important remedy to circumvent Pauli blocking completely was found in first associating pairs of ultracold fermionic atoms into weakly bound thermal molecules. As composite Bosons, these particles do not obey the Pauli exclusion principle, and can therefore be evaporatively cooled into a Bose-Einstein condensate using conventional techniques. Creating and manipulating such molecules will be the topic of the following section.

Diagnostics, Temperature Measurements The most important observables in studying ultracold Fermi gases are, as for BECs, density distributions of the cloud, that are obtained through imaging with resonant light. Very common is the measurement of the density distribution or after a certain time-of-flight to infer information on the momentum distribution of the gas, or the mean field energy stored in the gas. Assuming that there are no collisions between the particles during the expansion, the distribution function 1.3 can be mapped as $f_{TOF}(\vec{r},\vec{p},t) = f(\vec{r} - (\vec{p}/m)t)$. The resulting density distribution is calculated for example in [52]. For long times of flight when the initial size of the cloud becomes irrelevant, the distribution only depends on the momentum of the particles and is therefore expected to remain spherical.

A precise fit to the shape of the expanded cloud will be necessary to measure temperatures well below the Fermi temperature, images with very low distortion have to be achieved. The same problem occurs of course in a BEC, when the temperature drops significantly below the critical temperature, and the condensate fraction approaches unity.

The typically used imaging techniques allow only to measure 2-D density distributions, where the density in one axis is being integrated over. To eliminate experimental noise and to reduce the fitting effort, it is common to also integrate the density along a second axis to obtain a 1-D distribution. To ob-

tain the respective fit functions, one needs to integrate Eq. 1.10, which can be easily done by using the sum definition of the polylogarithmic function.

1.4 Interactions

Just as for BECs, interactions play an important role for the preparation, and for the physics of ultracold Fermi gases. In both cases, sufficient elastic collision rates are key to successful evaporative cooling. For a typical BEC in a trap that is well approximated by the Thomas-Fermi limit, the kinetic energy can be neglected, and the ground state can be described by a mean field interaction. An ultracold Fermi gas always has a finite kinetic energy due to the Pauli exclusion principle and the resulting Fermi motion of the particles. As a consequence, the momentum of the particles can never be neglected, significantly complicating the description. This means that in a weakly interacting gas, where $na^3 \ll 1$, the resulting mean field will be a small perturbation on the noninteracting state, aside from the case of weak attraction at extremely low temperatures, where the gas undergoes a transition into a superfluid BCS-state.

1.4.1 Collisions

Scattering of ultracold identical Fermions differs fundamentally from scattering of bosons, because their symmetry properties cause *s*-wave collisions to be forbidden while for bosons they are enhanced by a factor of two compared to nonidentical particles. Therefore, for identical Fermions, collisions necessarily need to involve angular momentum. However, such collisions are suppressed at low scattering energies [58], limiting their use in ultracold atoms experiments. In fact, the absence of *s*-wave collisions provided the opportunity to observe suppression of *p*-wave collisions, as a first demonstration of the fermionic properties of an ultracold Fermi gas [18]: As a spin-polarized gas of ^{40}K atoms was cooled down as shown in Fig. 1.4, the textbook result that the cross section for p-wave collisions should be $\sigma_p \propto E^2$ could be beautifully demonstrated.

1.4.2 Weakly Attractive Fermions, Superfluidity

While typical BECs are governed by their mean field interaction, the situation is totally different for a typical gas of Fermions at ultracold temperatures. To estimate the effect of weak interactions of a two-component Fermi gas at zero

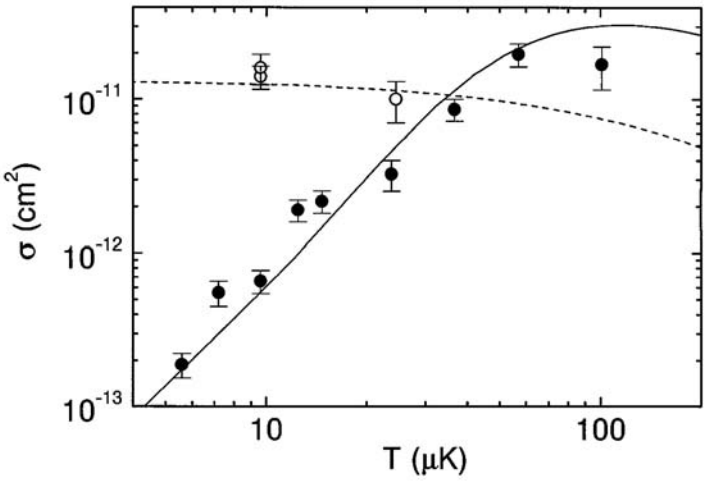

Fig. 1.4 Observation of the p-wave threshold law: Collision cross section as a function of temperature for a spin-polarized gas (solid points), and for a spin-mixture where s-wave scattering lead to a constant cross section. Reprinted figure with permission from B. deMarco et al., Phys. Rev. Lett. **82**,4208, 1999. ©1999 by the American Physical Society

temperature, let us estimate the ratio of mean field energy

$$E_{int} = gn = \frac{4\pi\hbar^2 a}{m} n \tag{1.16}$$

at the peak density $n(0)$ versus the Fermi energy assuming the density distribution of a noninteracting Fermi gas. The result is

$$\frac{E_{int}(n(0))}{E_F(a=0)} = 2\left(\frac{n(0)}{36\pi}\right)^{1/3} a = \frac{1}{6\pi} k_F a, \tag{1.17}$$

which has been calculated using Eqs. 1.6 and 1.8. Obviously, the dimensionless parameter $k_F a$ determines the interaction strength. For a typical dilute ultracold gas, where the interparticle separation is much larger than the scattering length ($na^3 \propto (k_F a)^3 \ll 1$), interactions will have only a small impact on the density profile. Obviously, this does not mean that the physics of such gases is not governed by their interactions. But because observing density and momentum distributions are the most important observables in ultracold atoms experiments, the consequences of such weak interactions are hard to spot. In fact, Bardeen, Cooper and Schrieffer (BCS) [3] were able to explain superconductivity in metals by an extremely weak attraction between the electrons, which causes the electrons to form delocalized pairs in momentum space called Cooper pairs [17]. The BCS theory successfully describes

Fermi systems with weak interactions, where the scattering length is much smaller than the interparticle spacing. At the same time, the mean distance between paired atoms is much larger than the interparticle separation. Associated with Cooper pairing is a gap in the excitation spectrum giving rise to the superfluid properties of the gas. At zero temperature, this gap has been calculated for a homogeneous two-component gas with *s*-wave interactions to be [25]

$$\Delta_0 = \frac{1}{2}\left(\frac{2}{e}\right)^{7/3} E_F \exp\left(-\frac{\pi}{2k_F|a|}\right). \tag{1.18}$$

The critical temperature for a transition into the superfluid state reads [12, 25]

$$T_{BCS} = \frac{e^{\gamma}}{\pi}\left(\frac{2}{e}\right)^{7/3} T_F \exp\left(-\frac{\pi}{2k_F|a|}\right) \approx 0.277 T_F \exp\left(-\frac{\pi}{2k_F|a|}\right), \tag{1.19}$$

where γ is Euler's constant. For typical values of $k_F|a|$, T_{BCS} is orders of magnitude lower than T_F. This means that still today, reaching the critical temperature in a BCS-type atomic gas with $k_F|a| \ll 1$ seems out of reach.

However, Eq. 1.19 also instructs us on how to achieve a higher critical temperature: With $k_F|a|$ approaching unity, Eq. 1.19 predicts T_{BCS} to be close to unity. Even though BCS theory is no longer valid for such strong interactions, increasing a has been the key to experimental success. Recent calculations estimate the critical temperature of a Fermi gas with infinite scattering length to be $T_C(a = \infty) \sim 0.2 T_F$ [8, 9].

1.4.3 Tunable Interactions, Feshbach Resonances

In the preceding section we have seen that it is desirable to increase the interaction strength in an ultracold Fermi gases. Near a Feshbach resonance the scattering length can be tuned to arbitrarily large positive or negative values by applying a suitable homogeneous magnetic field. $k_F a$ can then become on the order of unity or even much larger.

Ever since the first observation of Feshbach resonances in ultracold atomic gases [36], researchers were wondering how to make use of the tunability of the scattering length in the vicinity of a Feshbach resonance, which in the first place seemed very difficult because of the presence of strong inelastic decay: As the scattering rate increased for two-body elastic collisions, the scattering rate for three-body collisions increased even more: As a consequence, molecule formation that causes trap loss is strongly enhanced. Researchers were also hoping to make use of the very weakly bound molecular state associated with a Feshbach resonance. Both of these dreams have become the foundations of research with ultracold Fermi gases, the tunability of the inter-

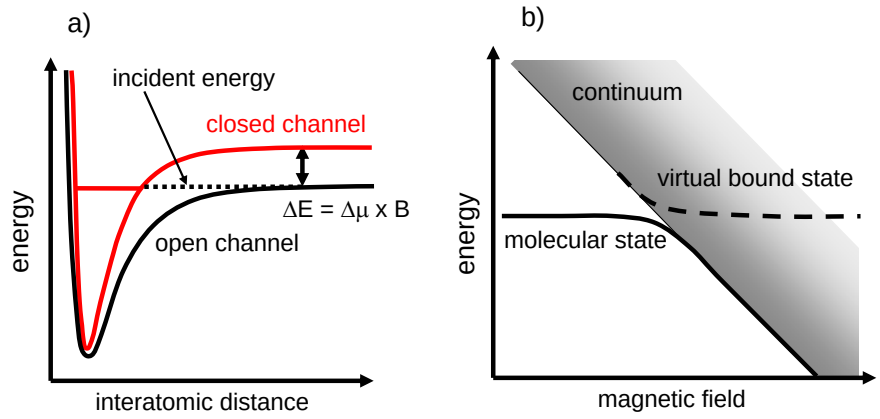

Fig. 1.5 a) A Feshbach resonance occurs, when a bound state of a closed channel is tuned into degeneracy with the continuum of the open scattering channel using an external magnetic field. b) The coupling of the two channels leads to an avoided crossing adiabatically connecting the molecular state with a free-atom state.

actions using Feshbach resonances was the key to all major achievements in the past years.

Feshbach Resonances The concept of Feshbach resonances has its roots in nuclear physics, where they were first studied by Herman Feshbach [23]. Here we give the reader an intuitive introduction into the concept of Feshbach resonances as they are being used in ultracold atoms experiments: Consider two ultracold atoms in a given Zeeman state scattering in their interatomic potential, which is usually called the open channel (Fig. 1.5 a)). For the same pair of atoms in different internal states, the potential can be different and represent so-called closed channels if their continuum lies above the incident scattering energy. When the atoms are scattered in the open channel, they may be coupled to the closed channel for example through hyperfine interactions. But as the continuum of the closed channel lies above the total energy, the atoms have to finally end up in the open channel, leading to a second-order coupling. If now the closed channel has a different magnetic moment than the open channel, the two potentials are tuned against each other by $\Delta E = \Delta\mu \times B$ by applying an external magnetic field B. Tuning a bound state in the closed channel into degeneracy with the continuum results in resonant scattering if there is a coupling between the two states. The scattering length can then be written in the form

$$a(B) = a_{bg}\left(1 + \frac{\Delta}{B - B_0}\right), \tag{1.20}$$

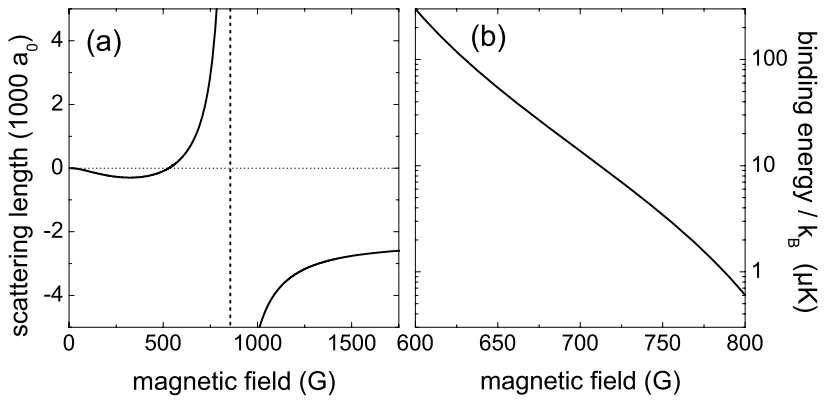

Fig. 1.6 Feshbach resonance for the two lowest spin states in ^6Li ($F = 1/2$, $m_F = \pm 1/2$ at low magnetic field): a) Scattering length versus the magnetic field. The resonance occurs at 834 G [4]. b) Binding energy of the molecular state associated with the Feshbach resonance.

where a_{bg} is the off-resonant background scattering length, Δ the width and B_0 the position of the resonance. As an example, Fig. 1.6 the scattering length versus the magnetic field is shown for the two lowest spin states in ^6Li. The coupling mixes the continuum of the open channel and the bound state in the closed channel to form two new states as shown in Fig. 1.5 b). In analogy to the avoided crossing in a two level system, the resulting molecular state is connected adiabatically to the free-atom continuum, when the closed channel is tuned into the continuum. This means that by adiabatically ramping the magnetic field across the resonance, pairs of atoms can be converted into molecules and vice versa. However, there is an important difference to the case of a simple two-level crossing as here, one of the states is a continuum state. This means that a stable molecular state can only exist below the continuum, while the molecular state embedded in the continuum can only be a virtual state.

Weakly Bound Molecules A resonantly large scattering length is caused by a bound molecular state that is very close to the continuum. When the scattering length is large and positive, there is a weakly bound state with a binding energy that can be calculated to be [40]

$$E_B = \frac{\hbar^2}{ma^2}. \tag{1.21}$$

This formula is correct as long as the scattering length is much larger than the effective range of the potential between the atoms, and the exact shape of the potential does not have an effect on the binding energy. This means that such molecules will always have a very tiny binding energy. Let us take as an example a molecule formed of two ^6Li atoms. Plugging in as the scattering length the effective range of the Lithium of $\sim$62.5 Bohr radii [65] and the mass of ^6Li into Eq. 1.21, one concludes that the binding energy of such a molecule needs to be much smaller than 10^{-6} eV, or 7 mK on the thermal energy scale of ultracold atoms. As an example, the binding energy of ^6Li Feshbach molecules is shown in the experimentally interesting range in Fig. 1.6. The size of such molecules has been calculated to be on the order of the scattering length a_{at} of the atoms, with on the order of 1000 Bohr radii an incredible size for a diatomic molecule. Accordingly, their scattering length is also very large, $a_{mol} = 0.6a_{at}$ [51].

On one hand these molecules have the very important advantage that their binding energy can be tuned freely by applying a magnetic field over the whole range of relevant energies for ultracold gases experiments, and all the molecules that share this weakly bound level are identical composite Bosons, even if their constituents are two Fermions. On the other hand, this particular molecular level is the highest in the molecular potential, and an enormous amount of potential energy, on the order of electronvolts, is stored in such a molecule, that could be released in molecule-molecule collisions, which would be an important loss channel in such a gas of molecules.

Enhancing elastic collision rates How large can the scattering cross section really get by increasing the scattering length? In the zero-energy limit, it is given by

$$\sigma_0 = 4\pi a^2 \tag{1.22}$$

for non-identical particles. So what happens near a Feshbach resonance, when the scattering length diverges? The scattering cross section can obviously not diverge. It is at most limited by the size of the wave packets of the colliding atoms, which is called the unitarity limit. The cross section is then $\sigma_u = 4\pi/k^2$, where k is the relative momentum of the colliding atoms. This value is approached when a becomes much larger than $1/k$. Note that this limit is still within the approximation that only s-wave collisions occur. At finite collision energies, the cross section can be described by

$$\sigma(k) = \frac{4\pi a^2}{1 + k^2 a^2}, \tag{1.23}$$

which interpolates between the zero-energy limit of Eq. 1.22 and the unitarity limit.

The first success of exploiting the tunability of interactions in an ultracold Fermi gas was the all-optical production of a degenerate Fermi gas [26] in J. Thomas' group at Duke University, where an optically trapped gas of ^6Li was exposed to an external magnetic field to increase the scattering length and thus the scattering cross section. This made it possible to achieve a collision rate high enough for efficient evaporative cooling.

Strong Interactions So far we've only been concerned with increasing the scattering rate through the scattering cross section. But what are the effects of resonant interactions on a deeply degenerate Fermi gas? Obviously, our estimation in Sec. 1.4.2 is no longer correct. In Eq. 1.16, we have to replace a by $1/k_F$ as a goes to infinity. This means that in this case, the interaction energy has to be proportional to $1/k_F \times n$. As $n \propto k_F^3$ (Eq. 1.7), we obtain

$$E_{int} \propto k_F^2 \propto E_F. \tag{1.24}$$

This indicates that the Fermi pressure will always scale in the same way as the attractive interaction strength between the particles. Indeed, a rigorous calculation shows that for infinite scattering length, the gas behaves much like a noninteracting Fermi gas with a chemical potential that is reduced by a factor of $(1+\beta)$ [2,31]. β can be shown to be a universal parameter that is the same for any Fermi system with infinite scattering length, independent of density or temperature. Such "universality" plays a role in many, very different Fermi systems, such as nuclei or neutron stars and has therefore been of great theoretical interest. Only recently the value of β was determined accurately using quantum Monte-Carlo calculations to be $\beta = -0.58 \pm 0.01$ [1,11]. Experimentally, β can be measured for example by a simple determination of the size of a cloud with infinite scattering length, as the density drops to zero now where $V(\vec{r}) = \mu(a \to \infty) = (1+\beta)E_F$.

The first realization of such a strongly interacting gas was achieved in John Thomas' group. The most striking result of their first measurements is shown in Fig. 1.7 [48]: Upon sudden release from the trap, the atoms expanded in an anisotropic way, reversing the initial aspect ratio of the trap. For a noninteracting gas, Eq. 1.7 tells us that we should expect an isotropic expansion independent of the trap potential. The fact that there was such a significant deviation from the noninteracting case could be attributed to a collisionless superfluid, but a classical description assuming a hydrodynamic expansion could explain such an expansion just as well. Nevertheless, this experiment provided the first presumptive evidence that ultracold Fermi gases were entering the superfluid regime.

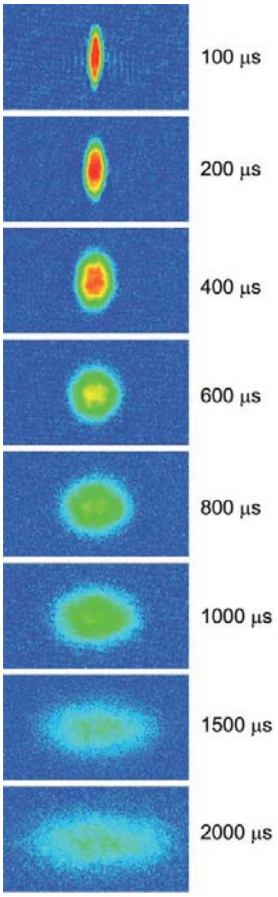

Fig. 1.7 Anisotropic expansion of a strongly interacting two-component Fermi gas. From Science **298**, 2179. Reprinted with permission from AAAS.

1.5 Feshbach Molecules and Molecular Condensates

1.5.1 Formation of Feshbach Molecules

Within a very short time after the first observation of molecules in the very weakly bound state of a Feshbach resonance [21], researchers established two ways to form such molecules efficiently:

- An adiabatic sweep from the side of the Feshbach resonance where no bound state exists to the side where the bound state appears binds previously unbound pairs of atoms into molecules [54].

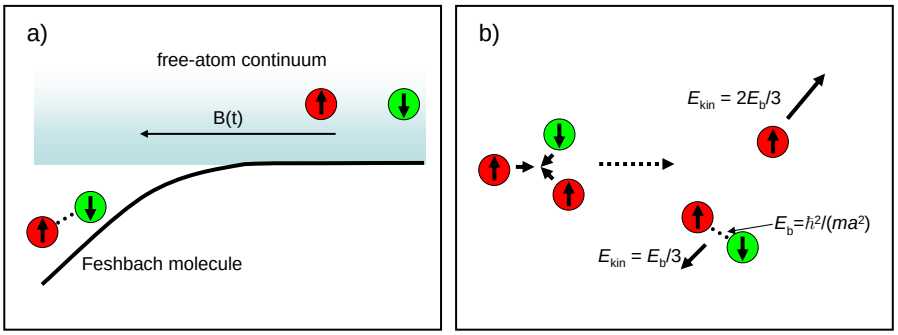

Fig. 1.8 The two most common ways to produce molecules from ultracold Fermions: a) A sweep of the magnetic field across the Feshbach resonance causes previously unbound atoms to be associated into molecules. This method is effective for highly degenerate samples. b) The magnetic field is held at a fixed value where three-body recombination is effective, and an atom-molecule chemical equilibrium is achieved. This method is effective for thermal samples, and when the molecules are collisionally stable.

- Three-body recombination leads to the binding of pairs of atoms into molecules. The binding energy is transferred into kinetic energy, and a chemical equilibrium of atoms and molecules is obtained [37].

Magnetic Field Ramps The very simple concept of creating molecules using an adiabatic magnetic field ramp across a Feshbach resonance is illustrated in Fig. 1.8 a): Free atom pairs on the right hand side of the figure, where no bound state exists, are adiabatically transferred into the emerging bound state on the resonance. While this concept has a lot in common with a well-known Landau-Zener two-level crossing, there exist some notable differences that arise primarily from the fact that the unbound atoms are not a single state, but two free atoms. This causes two main factors to influence the conversion efficiency of atoms into molecules: First, the magnetic field ramp has to be slow enough such that the spatial two-particle wave function can follow adiabatically into the bound state. In some cases this is difficult to realize experimentally, when strong inelastic collision processes limit the lifetime of the gas near the Feshbach resonance, and a compromise for the ramp speed optimizing the conversion efficiency has to be found. Second, the temperature of the atomic gas determines how many atoms will actually find themselves in a bound state, when the resonance is crossed. This means that for the conversion process to be highly effective, one needs to start with a highly degenerate gas of atoms. A detailed experimental study of this technique can be found in Ref. [33].

Three-Body Recombination Two free particles cannot simply bind into a molecule during a binary collision, because energy and momentum cannot be conserved at the same time: There has to be a third particle that takes away part of the binding energy as kinetic energy, such as a photon, or in our case a third atom.

The concept of the formation process is again very simple. The weakly bound molecular state is just one more energetically accessible state for the atoms, and while atoms are bound into molecules through collisions, releasing kinetic energy, molecules can also be dissociated into atoms again, provided enough kinetic energy is available to overcome the binding energy: A chemical equilibrium establishes in which the ratio of atoms bound into molecules versus free atoms is determined by the temperature of the gas and the binding energy of the molecules.

Three-Body Recombination of a Spin Mixture of Fermions While the Feshbach molecules we are concerned with here are made up of two atoms in different spin states, the third atom involved will necessarily have to be identical to one of the atoms forming the molecule. As at ultralow collision energies there is no angular momentum involved, the spatial wave function of the three colliding atoms is symmetric, forcing the spin part of the wave function to be antisymmetric. This cannot be achieved as soon as two identical particles are involved, so in this simple picture three-body recombination should be forbidden. Furthermore, as these Feshbach molecules occupy the highest vibrational level in the molecular potential, rapid collisional decay is expected to occur when the molecules exchange their internally stored energy for kinetic energy. Surprisingly enough, three-body recombination into the high-lying Feshbach molecular state proceeds at a high rate constant while the relaxation into lower-lying vibrational states is suppressed especially well for ^6Li atoms in the two lowest Zeeman levels. This phenomenon could be quantitatively explained by D. Petrov et al. [51]. Intuitively, their calculation can be understood by the fact that the size of the Feshbach molecule is on the order of the scattering length, typically much larger than the effective range R_e of the molecular potential. However, all other levels in the molecular potential are much more strongly confined, their size being on the order of R_e. For a relaxation to occur, two identical particles now have to come very close to each other, and then the argument holds that we mentioned earlier that all three-body recombination in a two-component Fermi gas should be suppressed by Pauli blocking.

Chemical Equilibrium The equilibrium ratio of molecules versus atoms in a thermal gas can be derived by minimizing the free energy of the system, which results in the so-called Saha equation, originally derived by Saha for a partially

ionized plasma [41]. Adapted to our case of a two-component gas, its reads

$$\frac{N_{mol}}{N_{at}} = \phi_{at} \times \exp\left(\frac{E_B}{k_B T}\right), \tag{1.25}$$

where N_{mol}, N_{at} are the number of molecules and atoms, respectively, ϕ_{at} is the atomic phase space density, and E_B is the molecular binding energy.

An important advantage of this technique is that a high conversion efficiency can be achieved even for gases that are far from being quantum degenerate, by choosing the binding energy to be much larger than the thermal energy in the gas. It turned out that a mixture of ^6Li-atoms and molecules can be very effectively cooled into degeneracy, due to the large elastic scattering cross sections for atom-atom-, atom-molecule-, and molecule-molecule collisions. Furthermore, Feshbach molecules see a trapping potential $U_{mol} = 2U_{at}$ twice as large as the atoms do when they are confined in a far-detuned optical dipole trap, which can be explained by the fact that both weakly bound atoms have the same polarizability as a free atom with respect to the far off resonant light. This leads to primarily atoms being evaporated from the trap, taking a kinetic energy of $U_{at} + \alpha k_B T$ with them, where alpha is a numerical constant of order unity [43]. Upon the loss of atoms, the atom molecule equilibrium needs to be readjusted, causing molecules to be dissociated, which absorbs kinetic energy. A more detailed description of this evaporative cooling scheme for a nondegenerate gas can be found in [14]. When the gas is cooled further and approaches degeneracy, there is a significant advantage over cooling a two-component Fermi gas because the bosonic molecules do not exhibit Pauli blocking and are cooled straight into a BEC, which will be discussed in the next section.

Detection of Feshbach Molecules One of the major difficulties in working with ultracold Feshbach molecules had been anticipated in their detection: How should it be possible to detect such a fragile object? What happens if they are exposed to resonant light?

All the methods that have been developed involve the dissociation of the molecules and the subsequent imaging of the resulting atoms. By far the simplest method is a ramp across the Feshbach resonance, where the molecules are dissociated into atoms, which are then imaged by conventional means. Obviously, this method as such cannot differentiate between atoms and molecules. To accomplish this, one can simply take two measurements, where in the first measurement, one performs the ramp across the resonance to dissociate the molecules, whereas in the second measurement it is omitted. The difference between the two measurements is then the number of atoms that had been bound into molecules [54]. Another way of differentiating between atoms and molecules is to separate atoms and molecules spatially in

a Stern-Gerlach type of experiment. Exploiting the fact that the molecules have a different magnetic moment than the atoms, they are accelerated at a different rate in an applied magnetic field gradient. After the molecules have been converted back into atoms, they appear at a different location as the atoms [32].

Beside a magnetic field ramp to dissociate the molecules one can also use radio frequency transitions in the following way: Consider the molecules are formed from atoms in two states, $|1\rangle$ and $|2\rangle$. Assume now a radio frequency field $\omega_{RF,at}$ can be applied to drive free atoms in $|2\rangle$ into a third state $|3\rangle$. If the atoms in $|2\rangle$ are bound into molecules, then an RF-transition from $|2\rangle$ to $|3\rangle$ at $\omega_{RF,at}$ cannot occur, as there is not exactly the same bound state between $|1\rangle$ and $|3\rangle$. However, by increasing the frequency of the RF pulse such that the binding energy of the molecule can be broken, the two bound atoms can be dissociated into two free atoms in $|1\rangle$ and $|3\rangle$, if the radio frequency $\omega_{RF,mol}$ of the pulse satisfies

$$\omega_{RF,mol} = \omega_{RF,at} + \frac{E_B}{\hbar}. \tag{1.26}$$

If now the radio frequency is tuned to $\omega_{RF,at}$, previously unbound atoms will be detected in state $|3\rangle$. If the radio frequency is tuned to $\omega_{RF,mol}$ however, no previously unbound atoms can detected, but molecules will be dissociated and previously bound atoms can be detected in $|3\rangle$. Using this method, also the binding energy can be determined from the radio frequency spectra [54]. Furthermore, the line shape of the spectra gives insight into the wave function of the molecules [15].

Yet another possibility to detect the molecules arises, when the atoms are very weakly bound: It turns out that when the size of the molecules is larger than the resonant wavelength, the individual atoms in the molecule "forget" that they are bound in a molecule and scatter photons as they would do as free atoms [67, 68]. Obviously, this is not a selective technique, one cannot differentiate between free atoms and bound molecules.

1.5.2 BEC of Molecules

The stable, weakly bound bosonic molecules produced from two fermionic atoms have a lot in common with Cooper pairs. The major difference is however that there does not exist a two-body bound state for the Cooper pairs, as their pairing mechanism is a many-body phenomenon. While the transition from a normal gas to a Cooper paired, superfluid Fermi gas is a very elusive effect that is very hard to observe in typical experimental observables like density or momentum distribution, the condensation of bosons is readily observed as a bimodal distribution in density and momentum. Therefore, it

was considered an important step towards a superfluid gas of Fermions, when molecular Bose-Einstein condensates could be produced [27, 38, 67].

At first sight, the properties of such molecular condensates do not differ very much from atomic condensates. In fact, these atoms can be perceived as bound pairs of an ion and its most loosely bound electron. The major difference lies in the fact that the interactions between the particles are much larger: The molecular gas becomes unstable against inelastic decay when the scattering length is reduced. In an atomic gas, three-body recombination as a loss process from the condensate increases sharply when the scattering length is increased, for example by approaching a Feshbach resonance. Thus, an atomic gas is generally restricted to the case where the scattering length is much smaller than the interparticle separation ($na^3 \ll 1$). For a molecular BEC, the regime of so-called strong interaction, where $na^3 \geq 1$ is easily reached. However, the system becomes complicated relatively quickly as the interaction strength is increased, because at the same time, the molecular binding energy is reduced, and soon happens to be on the same order of magnitude as other relevant energies of the system, so the two body nature of the molecules can no longer be ignored.

From the very beginning, there were two successful techniques for the preparation of molecular BECs, based on the two methods to produce Feshbach molecules: A sweep across a Feshbach resonance starting from a highly degenerate Fermi Sea, and the simple evaporative cooling of a spin mixture of fermionic atoms, leading first to the formation of ultracold molecules that finally condense into a BEC.

A Molecular BEC out of a Fermi Sea For this technique to work, one starts with a very cold Fermi gas of atoms and assumes that when changing the magnetic field slowly enough while crossing the Feshbach resonance, the process of molecule formation is adiabatic and the entropy of the ensemble is conserved. To calculate the required temperature of the Fermi gas to obtain a molecular BEC, one can compare the entropy on both sides of the resonance, as has been done in Ref. [12],

$$S_{Fermi} = k_B N \pi^2 \frac{T}{T_F}, \tag{1.27}$$

$$S_{BEC} = k_B N_{mol} \frac{2\pi^4}{45\zeta(3)} \left(\frac{T}{T_{BEC}} \right)^3, \tag{1.28}$$

ζ is the Riemann zeta function and T_{BEC} is the critical temperature for BEC. For simplicity we have omitted all effects of interactions. Setting $T/T_{BEC} = 1$ $S_{Fermi} = S_{BEC}$, and $N = 2N_{mol}$, we get

$$\frac{T}{T_F} = \frac{\pi^2}{45\zeta(3)} \approx 0.18. \tag{1.29}$$

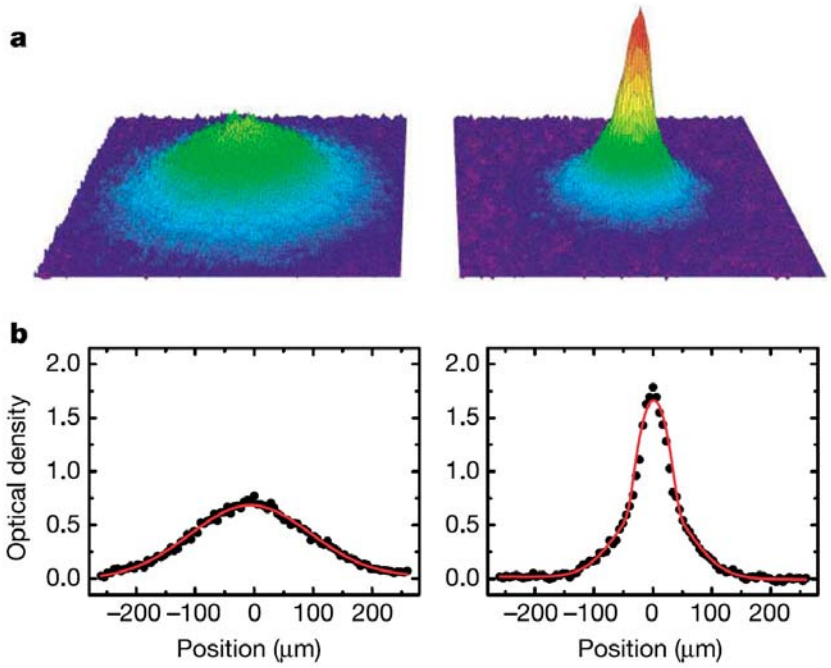

Fig. 1.9 Time-of-flight images of $^{40}K_2$-molecules created through a magnetic field ramp across a Feshbach resonance. The image on the left shows molecules that have been created from Fermions at 0.19 T_F, very close to the critical temperature. For the image on the right, Fermions at 0.06 T_F were employed. Here, a clearly visible bimodal distribution proves the presence of a molecular BEC. Reprinted by permission from Macmillan Publishers Ltd: Nature **426**, 537, © 2003

This is a readily achievable value in most ultracold Fermion experiments, and indeed it is very close to the temperature at which the critical temperature for Bose condensation was observed in the first molecular BEC experiment in the group of D. Jin [27] with ^{40}K-atoms. Time-of-flight images of this experiment are shown in Fig. 1.9. The image on the left shows the momentum distribution of molecules that have been created from a Fermi gas with a temperature of 0.19 T_F. No bimodal profile as a signature of a BEC is visible, but a temperature fit to this image reveals $T = 290\,\text{nK}$, which corresponds to $\sim 0.9\,T_{BEC}$, well in agreement with the expectation. The image on the right was taken of molecules that were created from Fermions at $0.06T_F$. These molecules show clearly the typical bimodal distribution of a BEC at about one half of the critical temperature. There was however one important difficulty that experimenters struggled with during these experiments. As inelastic collisions among the trapped ^{40}K atoms and molecules significantly reduced the life-

time, the adiabaticity condition for the magnetic field sweep was very difficult to achieve without sacrificing most of the particles.

A Molecular BEC by Direct Evaporation of Thermal Fermions While creating a molecular BEC using the previously described technique requires the prior preparation of a highly degenerate Fermi gas, creating a molecular BEC from thermal molecules can be much more efficient, as there is no Pauli blocking that obstructs thermalization in the final evaporative cooling stage. The major prerequisite for this technique to work is a sufficient collisional stability of the Feshbach molecules, which so far has only been achieved with ^6Li atoms. The most significant advantage is that through evaporative cooling it is typically possible to achieve temperatures significantly below the critical temperature for BEC. Assuming that one can ramp the magnetic field to the Fermi side of the Feshbach resonance without increasing the entropy, extremely cold Fermi gases can be produced: Assuming a realistic temperature of the BEC of $T_{BEC}/4$, the temperature of the Fermi gas estimated using Eqs. 1.27 and 1.28 is $3 \times 10^{-3}\, T_F$! As we haven't included interactions in our crude estimation, which are important for the molecular BEC with its large scattering length, the final temperature will be slightly higher [12]. The prospect for such low temperatures cause molecular BECs made from ^6Li attractive starting points for experiments with ultracold Fermions.

1.6 BEC-BCS Crossover

indexBEC-BCS crossover In the previous section we have seen two techniques to produce a BEC of molecules: The first one involves an adiabatic crossing of a Feshbach resonance to create a gas of superfluid bosons from a highly degenerate Fermi sea. We quoted the second technique as an ideal starting point to produce a deeply degenerate Fermi gas starting from a Bose gas. But what exactly happens when the gas undergoes this crossover from a Fermi gas to a BEC, and vice versa?

1.6.1 From Fermions to Bosons, a Continuous Crossover!

The theoretical exploration of this question already has a long history. While Eagles initiated the idea that increasing the effective attraction between electrons leads to strongly bound pairs that condense into a BEC in 1969 [22], Leggett found a direct link between "diatomic molecules and Cooper pairs" [42], and Nozières and Schmitt-Rink concluded in 1985 that "the transition from weak coupling to strong coupling superconductivity is smooth" [47]. Hence,

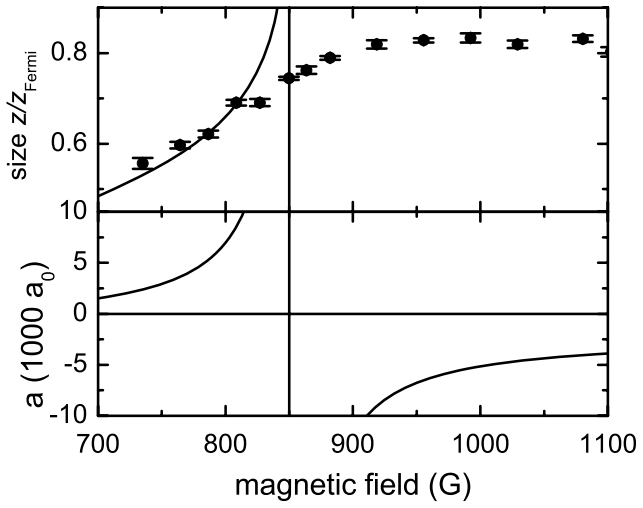

Fig. 1.10 Size of an ultracold gas of ^6Li atoms in the BEC-BCS crossover, normalized to the size of a noninteracting fermi gas: On the Bose side of the Feshbach resonance, the size initially follows the expectation for an interacting BEC (solid line), then it levels off and reaches the size of a strongly interacting Fermi gas. The bottom part of the graph shows the corresponding scattering length for reference (figure adapted from [6]).

all these ideas had been developed long before one could think of realizing such systems with ultracold atoms using Feshbach resonances. An excellent theoretical overview is given in Ref. [13]

So what exactly happens while a Bose gas is transformed into a Fermi gas? After all, the quantum statistics of the gas is completely altered! It turned out that there is no discontinuity in any observable of the system, and so far all experiments confirm this conclusion. In fact, researchers were impressed that an ultracold cloud of ^6Li atoms could be transformed from a molecular BEC into an interacting Fermi gas and back without any noticeable increase in temperature, strengthening the assumption of the previous section that the Feshbach resonance can be crossed in an isentropic way [5]. The density distribution of the gas evolved continuously from an interacting BEC into an interacting Fermi gas (see Fig. 1.10).

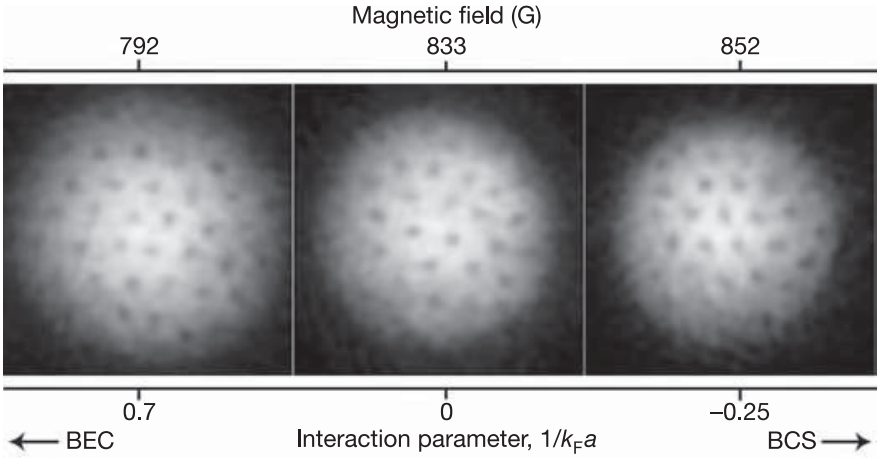

Fig. 1.11 Vortex lattices in a gas of ^6Li atoms in the BEC-BCS crossover. On the left, the magnetic field is tuned below the Feshbach resonance ($a > 0$), resulting in a molecular BEC. In the middle, the magnetic field is tuned on resonance ($a \to \infty$). For the image on the right, the scattering length is negative, and no two-body bound state is available. Reprinted by permission from Macmillan Publishers Ltd: Nature **435**, 1047, © 2005.

1.6.2 High-T_C-Superfluidity in a Fermi Gas of Atoms

The prospect of being able to realize ultracold Fermi gases with resonant interactions triggered a tremendous theoretical interest in the topic. Superfluidity was suggested to occur at very high temperatures, "resonance superfluidity" with a critical temperature on the order of the Fermi temperature [34, 49, 62].

When the first molecular Bose-Einstein condensates were realized, this immediately raised the question, under which circumstances such a gas would remain superfluid, when the binding energy of of the molecules is reduced further and further, and finally, after crossing the Feshbach resonance, when there is no two-body bound state any more. But how could one observe a clear signature for condensation, in a similar way as the observation of a bimodal distribution that occurs during Bose condensation?

Taking the original idea of Eagles [22] of many-body pairs that Bose condense seriously, one should expect that those pairs should exhibit a bimodal momentum distribution below the critical temperature. Such a momentum distribution should manifest itself in time-of-flight measurements of the density after a sudden switch-off of the trap. The situation is complicated however by the fact that the expansion is governed by the strong interaction between the particles. Also, the delicate pairs are immediately dissociated when

the density is reduced. However, researchers were quick to find a solution to these difficulties: Using a magnetic field ramp to the molecule side of the Feshbach resonance, quick enough to make sure collisions between the particles do not lead to thermalization between the particles, such that the resulting molecules would not find the time to arrange themselves in a BEC, but slow enough such that pairs of Fermions would adiabatically be projected into molecules. Then, a time-of-flight expansion of the gas should reflect the momentum distribution of the many-body pairs that exist in the crossover region. Conceptually, such experiments were a minor modification of the way how molecular condensates were produced in Ref. [27] from ^{40}K-atoms: A Fermi gas was produced with a certain temperature. Then, the magnetic field was ramped to a specific value within the crossover, slowly enough that the ramp was adiabatic with respect to the many-body system. To determine now the momentum distribution of the pairs at this particular magnetic field, a fast ramp was applied to the molecule side of the Feshbach resonance. The momentum distribution was then determined as before using time-of-flight absorption imaging. The result was stunning: Pairs of fermions could be seen to be condensed within the whole crossover region [53], with both the number of condensed pairs and the critical temperature being largest close to the Feshbach resonance. The major difficulty of this so-called projection technique lies in the fact that the time scale for the many-body system to evolve adiabatically has to be significantly longer than the time scale for pairs to form tightly bound molecules. However, the initial results were quickly confirmed using ^{6}Li atoms [70], complemented with systematic tests that showed that the projection technique works as envisioned. Together with measurements on the collective dynamics of strongly interacting, ultracold ^{6}Li gases, these results were considered to prove the existence of a superfluid phase on both sides of the Feshbach resonance at sufficiently low temperature. However, an unambiguous, direct manifestation of a superfluidity had not been observed. Eventually, this has been achieved by M. Zwierlein et al. [66] who succeeded to observe vortices in a rotating gas of ^{6}Li atoms. Images of such rotating clouds are shown in Fig. 1.11 for different magnetic fields, below the Feshbach resonance where there is a two-body bound state supported (left), on resonance (middle), and finally, where bosonic pairs can only be formed in a many-body context above the Feshbach resonance.

1.7 Conclusion

Within less than a decade since the first successful experiments on ultracold Fermi gases, a whole new community developed that now has at its disposal Fermi superfluids with tunable interactions. In fact, this tunability reaches

all the way from a weakly interacting BCS-type of gas with completely delocalized pairs via a strongly interacting Fermi gas with diverging scattering length, where the gas shows a universal behavior to a Bose-condensed gas of molecules. These gases now serve as an ideal starting point to study both long-standing questions from other fields of physics as well as completely new phenomena: The physics of unbalanced spin mixtures has been a lively debated topic during the past years [50,69], as well as collective dynamics [16,64]. Ultracold Fermi gases serve as an ideal model system for solid state physics, in tailored optical potentials such as lattices [55, 57], combined with tunable interactions [39, 46]. Methods from nuclear physics are being applied to cold Fermi gases, and vice versa [2]. High-energy physicists realize that ultracold Fermions can help to better understand Quark-Gluon Plasma [59]. An excellent overview over current research topics will be given in Ref. [35].

References

1 G. E. Astrakharchik, J. Boronat, J. Casulleras, , and S. Giorgini. Equation of State of a Fermi Gas in the BEC-BCS Crossover: A Quantum Monte Carlo Study. *Physical Review Letters*, 93(20):200404, 2004.

2 George A. Baker. Neutron matter model. *Phys. Rev. C*, 60:054311, Oct 1999.

3 J. Bardeen, L. N. Cooper, and J. R. Schrieffer. Theory of Superconductivity. *Phys. Rev.*, 108(5):1175, Dec 1957.

4 M. Bartenstein, A. Altmeyer, S. Riedl, R. Geursen, S. Jochim, C. Chin, J. Hecker Denschlag, R. Grimm, A. Simoni, E. Tiesinga, C. J. Williams, and P. S. Julienne. Precise Determination of ^{6}Li Cold Collision Parameters by Radio-Frequency Spectroscopy on Weakly Bound Molecules. *Physical Review Letters*, 94(10):103201, 2005.

5 M. Bartenstein, A. Altmeyer, S. Riedl, S. Jochim, C. Chin, J. Hecker Denschlag, and R. Grimm. Crossover from a Molecular Bose-Einstein Condensate to a Degenerate Fermi Gas. *Phys. Rev. Lett.*, 92(12):120401, March 2004.

6 Markus Bartenstein. *From Molecules to Cooper Pairs: Experiments in the BEC-BCS crossover*. PhD thesis, Universität Innsbruck, 2005.

7 C. C. Bradley, C. A. Sackett, and R. G. Hulet. Bose-Einstein condensation of lithium: Observation of limited condensate number. *Phys. Rev. Lett.*, 78(6):985, February 1997.

8 Aurel Bulgac, Joaquin E. Drut, and Piotr Magierski. Spin 1/2 Fermions in the Unitary Regime: A Superfluid of a New Type. *Physical Review Letters*, 96(9):090404, 2006.

9 Evgeni Burovski, Nikolay Prokof'ev, Boris Svistunov, and Matthias Troyer. Critical Temperature and Thermodynamics of Attractive Fermions at Unitarity. *Physical Review Letters*, 96(16):160402, 2006.

10 D. A. Butts and D. S. Rokhsar. Trapped Fermi gases. *Phys. Rev. A*, 55(6):4346, June 1997.

11 J. Carlson, S.-Y. Chang, V. R. Pandharipande, and K. E. Schmidt. Superfluid Fermi Gases with Large Scattering Length. *Phys. Rev. Lett.*, 91(5):050401, July 2003.

12 L. D. Carr, G.V. Shlyapnikov, and Y. Castin. Achieving a BCS Transition in an Atomic Fermi Gas. *Phys. Rev. Lett.*, 92(15):150404, April 2004.

13 Qijin Chen, Jelena Stajic, Shina Tan, and K. Levin. BCS-BEC crossover: From high temperature superconductors to ultracold superfluids. *Physics Reports*, 412(1):1–88, June 2005.

14 Cheng Chin and Rudolf Grimm. Thermal equilibrium and efficient evaporation of an ultracold atom-molecule mixture. *Phys. Rev. A*, 69:033612, March 2004.

15 Cheng Chin and Paul S. Julienne. Radio-frequency transitions on weakly bound ultracold molecules. *Physical Review A (Atomic, Molecular, and Optical Physics)*, 71(1):012713, 2005.

16 Bason Clancy, Le Luo, and John E. Thomas. Observation of Nearly Perfect Irrotational Flow in Normal and Superfluid Strongly Interacting Fermi Gases. *Physical Review Letters*, 99(14):140401, 2007.

17 Leon N. Cooper. Bound Electron Pairs in a Degenerate Fermi Gas. *Phys. Rev.*, 104(4):1189–1190, Nov 1956.

18 B. DeMarco, J. L. Bohn, J. P. Burke, Jr., M. Holland, and D. S. Jin. Measurement of *p*-wave threshold law using evaporatively cooled fermionic atoms. *Phys. Rev. Lett.*, 82(21):4208, May 1999.

19 B. DeMarco and D. S. Jin. Onset of Fermi degeneracy in a trapped atomic gas. *Science*, 285(5434):1703, September 1999.

20 B. DeMarco, S. B. Papp, and D. S. Jin. Pauli blocking of collisions in a quantum degenerate atomic Fermi gas. *Phys. Rev. Lett.*, 86(24):5409, June 2001.

21 Elizabeth A. Donley, Neil R. Claussen, Sarah T. Thompson, and Carl E. Wieman. Atom-molecule coherence in a Bose-Einstein condensate. *Nature*, 417:529, May 2002.

22 D. M. Eagles. Possible Pairing without Superconductivity at Low Carrier Concentrations in Bulk and Thin-Film Superconducting Semiconductors. *Phys. Rev.*, 186(2):456, Oct 1969.

23 Herman Feshbach. A Unified Theory of Nuclear Reactions. *Ann. Phys.*, 5:337, 1958.

24 Takeshi Fukuhara, Yosuke Takasu, Mitsutaka Kumakura, and Yoshiro Takahashi. Degenerate Fermi Gases of Ytterbium. *Physical Review Letters*, 98(3):030401, 2007.

25 L. P. Gorkov and T. K. Melik-Barkhudarov. Contribution to the theory of superfluidity in an imperfect Fermi gas. *Sov. Phys. JETP*, 13:1018, 1961.

26 S. R. Granade, M. E. Gehm, K. M. O'Hara, and J. E. Thomas. All-optical production of a degenerate Fermi gas. *Phys. Rev. Lett.*, 88(12):120405, March 2002.

27 M. Greiner, Cindy A. Regal, and D. S. Jin. Emergence of a molecular Bose-Einstein condensate from a Fermi gas. *Nature*, 426:540, Nov 2003.

28 R. Grimm, M. Weidemüller, and Y. Ovchinnikov. Optical dipole traps for neutral atoms. *Adv. At. Mol. Opt. Phys.*, 42, 2000.

29 Z. Hadzibabic, S. Gupta, C. A. Stan, C. H. Schunck, M. W. Zwierlein, K. Dieckmann, and W. Ketterle. Fiftyfold Improvement in the Number of Quantum Degenerate Fermionic Atoms. *Phys. Rev. Lett.*, 91(16):160401, Oct 2003.

30 Z. Hadzibabic, C. A. Stan, K. Dieckmann, S. Gupta, M. W. Zwierlein, A. Görlitz, and W. Ketterle. Two-Species Mixture of Quantum Degenerate Bose and Fermi Gases. *Phys. Rev. Lett.*, 88(16):160401, Apr 2002.

31 Henning Heiselberg. Fermi systems with long scattering lengths. *Phys. Rev. A*, 63(4):043606, Mar 2001.

32 Jens Herbig, Tobias Kraemer, Michael Mark, Tino Weber, Cheng Chin, Hanns-Christoph Nägerl, and Rudolf Grimm. Preparation of a Pure Molecular Quantum Gas. *Science*, 301:1510–1513, August 2003.

33 E. Hodby, S. T. Thompson, C. A. Regal, M. Greiner, A. C. Wilson, D. S. Jin, E. A. Cornell, and C. E. Wieman. Production Efficiency of Ultracold Feshbach Molecules in Bosonic and Fermionic Systems. *Physical Review Letters*, 94(12):120402, 2005.

34 M. Holland, S. J. J. M. F. Kokkelmans, M. L. Chiofalo, and R. Walser. Resonance superfluidity in a quantum degenerate Fermi gas. *Phys. Rev. Lett.*, 87(12):120406, September 2001.

35 M. Inguscio, W. Ketterle, and C. Salomon, editors. *Ultracold Fermi Gases.* Proceedings of the International School of Physics "Enrico Fermi", Course CLXIV, Varenna, 20-30 June 2006, IOS, Amsterdam (to be published), 2007.

36 S. Inouye, M. R. Andrews, J. Stenger, H.-J. Miesner, D. M. Stamper-Kurn, and W. Ketterle. Observation of Feshbach resonances in a Bose-Einstein condensate. *Nature*, 392(0):151, March 1998.

37 S. Jochim, M. Bartenstein, A. Altmeyer, G. Hendl, C. Chin, J. Hecker Denschlag, and R. Grimm. Pure Gas of Optically Trapped Molecules Created from Fermionic Atoms. *Phys. Rev. Lett.*, 91(24):240402, Dec 2003.

38 S. Jochim, M. Bartenstein, A. Altmeyer, G. Hendl, S. Riedl, C. Chin, J. Hecker Denschlag, and R. Grimm. Bose-Einstein Condensation of Molecules. *Science*, 301:2101–2103, Nov 2003.

39 Michael Köhl, Henning Moritz, Thilo Stöferle, Kenneth Günter, and Tilman Esslinger. Fermionic Atoms in a Three Dimensional Optical Lattice: Observing Fermi Surfaces, Dynamics, and Interactions. *Physical Review Letters*, 94(8):080403, 2005.

40 L. D. Landau and E. M. Lifshitz. *Quantum Mechanics: Non-Relativistic Theory*. Pergamon Press, Oxford, 3rd ed. edition, 1977.

41 L. D. Landau and E. M. Lifshitz. *Statistical Physics, Part 1*. Pergamon Press, Oxford, 3rd ed. edition, 1980.

42 A. J. Leggett. Diatomic Molecules and Cooper Pairs. In A. Pekalski and R. Przystawa, editors, *Modern Trends in the Theory of Condensed Matter*, pages 13–27. Springer-Verlag, Berlin, 1980.

43 O. J. Luiten, M. W. Reynolds, and J. T. M. Walraven. Kinetic theory of the evaporative cooling of a trapped gas. *Phys. Rev. A*, 53(1):381, January 1996.

44 J. M. McNamara, T. Jeltes, A. S. Tychkov, W. Hogervorst, and W. Vassen. Degenerate Bose-Fermi Mixture of Metastable Atoms. *Physical Review Letters*, 97(8):080404, 2006.

45 Marc-Oliver Mewes, Gabriele Ferrari, Florian Schreck, Alice Sinatra, and Christophe Salomon. Simultaneous magneto-optical trapping of two lithium isotopes. *Phys. Rev. A*, 61(1):011403, Dec 1999.

46 Henning Moritz, Thilo Stöferle, Kenneth Günter, Michael Köhl, and Tilman Esslinger. Confinement Induced Molecules in a 1D Fermi Gas. *Physical Review Letters*, 94(21):210401, 2005.

47 P. Nozières and S. Schmitt-Rink. Bose condensation in an attractive fermion gas: From weak to strong coupling superconductivity. *Phys. Rev.*, 186(2):456–463, Oct 1969.

48 K. M. O'Hara, S. L. Hemmer, M. E. Gehm, S. R. Granade, and J. E. Thomas. Observation of a strongly interacting degenerate Fermi gas of atoms. *Science*, 298:2179, December 2002.

49 Y. Ohashi and A. Griffin. BCS-BEC crossover in a gas of Fermi atoms with a Feshbach resonance. *Phys. Rev. Lett.*, 89(13):130402, September 2002.

50 G. B. Partridge, Wenhui Li, Y. A. Liao, R. G. Hulet, M. Haque, and H. T. C. Stoof. Deformation of a Trapped Fermi Gas with Unequal Spin Populations. *Physical Review Letters*, 97(19):190407, 2006.

51 D.S. Petrov, C. Salomon, and G.V. Shlyapnikov. Weakly bound dimers of fermionic atoms. *Phys. Rev. Lett.*, 93:090404, Aug 2004.

52 Lev Pitaevskii and Sandro Stringari. *Bose-Einstein Condensation*. Oxford University Press, 2003.

53 C. A. Regal, M. Greiner, and D. S. Jin. Observation of Resonance Condensation of Fermionic Atom Pairs. *Phys. Rev. Lett.*, 92(4):040403, Jan 2004.

54 Cindy A. Regal, Christopher Ticknor, John L. Bohn, and Deborah S. Jin. Creation of ultracold molecules from a Fermi gas of atoms. *Nature*, 424:47, July 2003.

55 G. Roati, E. de Mirandes, F. Ferlaino, H. Ott, G. Modugno, and M. Inguscio. Atom Interferometry with Trapped Fermi Gases. *Physical Review Letters*, 92(23):230402, 2004.

56 G. Roati, F. Riboli, G. Modugno, and M. Inguscio. Fermi-Bose Quantum Degenerate $^{40}K - ^{87}$ *Rb* Mixture with Attractive Interaction. *Phys. Rev. Lett.*, 89(15):150403, Sep 2002.

57 T. Rom, Th. Best, D. van Oosten, U. Schneider, S. Fölling, B. Paredes, and I. Bloch. Free fermion antibunching in a degenerate atomic Fermi gas released from an optical lattice. *Nature*, 444:733, 2006.

58 J. J. Sakurai. *Modern Quantum Mechanics*. Addison-Wesley, revised edition, 1994.

59 T. Schäfer. What atomic liquids can teach us about quark liquids. In *Proceedings of the Yukawa International Seminar 2006 "New Frontiers in QCD"*.

60 F. Schreck, L. Khaykovich, K. L. Corwin, G. Ferrari, T. Bourdel, J. Cubizolles, and C. Salomon. Quasipure Bose-Einstein Condensate Immersed in a Fermi Sea. *Phys. Rev. Lett.*, 87(8):080403, Aug 2001.

61 C. Silber, S. Günther, C. Marzok, B. Deh, Ph. W. Courteille, and C. Zimmermann. Quantum-Degenerate Mixture of Fermionic Lithium and Bosonic Rubidium Gases. *Physical Review Letters*, 95(17):170408, 2005.

62 Eddy Timmermans, Kyoko Furuya, Peter W. Milonni, and Arthur K. Kerman. Prospect of creating a composite Fermi-Bose superfluid. *Phys. Lett. A*, 285:228, 2001.

63 Andrew G. Truscott, Kevin E. Strecker, William I. McAlexander, Guthrie B. Partridge, and Randall G. Hulet. Observation of Fermi pressure in a gas of trapped atoms. *Science*, 291(5513):2570, March 2001.

64 M. J. Wright, S. Riedl, A. Altmeyer, C. Kohstall, E. R. Sanchez Guajardo, J. Hecker Denschlag, and R. Grimm. Finite-Temperature Collective Dynamics of a Fermi Gas in the BEC-BCS Crossover. *Physical Review Letters*, 99(15):150403, 2007.

65 Zong-Chao Yan, James F. Babb, A. Dalgarno, and G. W. F. Drake. Variational calculations of dispersion coefficients for interactions among H, He, and Li atoms. *Phys. Rev. A*, 54(4):2824, Oct 1996.

66 M. W. Zwierlein, J. R. Abo-Shaeer, A. Schirotzek, C. H. Schunck, and W. Ketterle. Vortices and superfluidity in a strongly interacting Fermi gas. *Nature*, 435:1047–1051, June 2005.

67 M. W. Zwierlein, C. A. Stan, C. H. Schunck, S. M. F. Raupach, S. Gupta, Z. Hadzibabic, and W. Ketterle. Observation of Bose-Einstein Condensation of Molecules. *Phys. Rev. Lett.*, 91(25):250401, Dec 2003.

68 Martin W. Zwierlein. *High-Temperature Superfluidity in an Ultracold Fermi Gas*. PhD thesis, Massachusetts Institute of Technology, 2006.

69 Martin W. Zwierlein, Andre Schirotzek, Christian H. Schunck, and Wolfgang Ketterle. Fermionic Superfluidity with Imbalanced Spin Populations. *Science*, 311(5760):492–496, 2006.

70 M.W. Zwierlein, C. A. Stan, C. H. Schunck, S. M. F. Raupach, A. J. Kerman, and W. Ketterle. Condensation of Pairs of Fermionic Atoms near a Feshbach Resonance. *Phys. Rev. Lett.*, 92(12):120403, March 2004.

Index